J. Fluid Mech. (1992), *vol.* 238, *pp.* 435–466
Printed in Great Britain

Velocity profile statistics in a turbulent boundary layer with slot-injected polymer

By A. A. FONTAINE, H. L. PETRIE AND T. A. BRUNGART
The Pennsylvania State University, Applied Research Laboratory, State College, PA 16804, USA

(Received 23 June and in revised form 21 October 1991)

The modification of a flat-plate turbulent boundary layer resulting from the injection of drag-reducing polymer solutions through a narrow inclined slot into the near-wall region of the flow has been studied. Two-component coincident laser-Doppler velocity profile measurements were taken with a free-stream velocity of 4.5 m/s with polymer injection, water injection, and no injection. Polyethylene oxide solutions at concentrations of 500 and 1025 w.p.p.m. were injected. These data are complemented by polymer concentration profile measurements that were taken using a laser-induced-fluorescence technique. Also, integrated skin friction measurements were made with a drag balance for a range of polymer injection conditions and free-stream velocities. The immediate effects of polymer injection are a deceleration of the flow near the wall, a dramatic decrease of the vertical r.m.s. velocity fluctuation levels and the Reynolds shear stress levels, and a mean velocity profile approaching Virk's asymptotic condition. These effects relax substantially with increasing streamwise distance from the injection slot and become similar to the effects observed for dilute homogeneous polymer flows.

1. Introduction

Skin friction reduction and turbulent boundary layer (TBL) modification by polymer additives has received considerable attention since discovery of the phenomenon by Toms (1949). Most of the research, to date, has been concerned with the effects of homogeneous polymer solutions in internal flows. Experiments have shown that polymer additives extend the buffer region of a TBL from the wall and reduce turbulent momentum transport significantly in the direction normal to the surface, see Reischman & Tiederman (1975) and Willmarth, Wei & Lee (1987). McComb & Rabie (1982) confirmed that drag reduction occurs when the polymer is present in the buffer region of the TBL, $11.6 < y^+ < 100$. The + superscript indicates normalization with wall variables, the friction velocity u^* and the kinematic viscosity ν; $y^+ = yu^*/\nu$. Tiederman, Luchik & Bogard (1985) reinforced this conclusion by measuring no skin friction reduction in a low-speed channel flow when the polymer was confined to the viscous sublayer of a TBL. Only after the polymer had diffused into the buffer region was skin friction reduction measured.

Despite extensive investigation, the detailed mechanisms of polymer skin friction reduction have yet to be explained conclusively. Thorough reviews on drag-reducing polymer additives, their effects on turbulent flows, and their industrial applications are presented by White & Hemmings (1976), Berman (1978), Sellin, Hoyt & Scrivener (1982*a*) and Sellin *et al.* (1982*b*).

One area of practical importance which has received less attention is polymer skin

friction reduction in external flows. In these flows, polymers are typically introduced into the near wall region of a TBL through narrow inclined slots. Wall injection systems have been studied in an attempt to optimize both the design, type and size of the injector, and the injection rates, see Wu & Tulin (1972) and Walker, Tiederman & Luchik (1986). These studies indicate that slot injectors should have a small injection angle with respect to the flow direction and injection rates should be of the same order of magnitude as the flow rate in the viscous sublayer. The flow rate in the viscous sublayer per unit span, Q_S, is defined in this discussion as the discharge per unit width of the TBL in the region $0 < y^+ \leqslant 11.6$, and is equal to 67.3ν, see Wu & Tulin (1972). For a given fluid and fluid temperature, this flow rate is a constant, independent of free-stream velocity or streamwise distance from the boundary-layer origin.

The use of polymer injection for skin friction reduction in external flows is complicated by the dependence of the performance of the polymer in reducing skin friction on the diffusion of the polymer away from the wall as it convects and mixes with the ambient fluid. The diffusion rate across the TBL of the polymer additive may be retarded substantially by the actions of the polymer compared with that of a passive contaminant. The direct coupling of the momentum and mass transfer aspects of the problem broaden the scope of what must be studied to understand the effects of the polymer additives.

The diffusion of a passive contaminant from a line source into a flat-plate TBL was investigated by Poreh & Cermak (1964). The diffusion process was described using a diffusion boundary-layer thickness, λ, defined as the distance from the wall at which the mean concentration drops to 50% of its maximum concentration at a given streamwise measurement location. Based on their mean concentration profile measurements, Poreh & Cermak (1964) identified four diffusion zones downstream of the injector: initial, intermediate, transition and final diffusion. In the initial zone, a concentrated layer of the injectant resides close to the wall and large concentration gradients exist. The diffusion boundary-layer thickness is on the order of or slightly larger than the momentum boundary-layer sublayer. Values of λ, normalized by the local momentum boundary-layer thickness δ, are less than 0.1 in this zone. In the case of a passive contaminant, the initial zone has not, to the authors' knowledge, been studied experimentally because it is too thin and too short.

The intermediate diffusion zone is typified by a diffusion boundary layer that is submerged in the momentum boundary layer but is large relative to the sublayer thickness of the momentum boundary layer. Values of λ/δ increase from 0.1 to 0.39 with increasing streamwise distance from the line source and the mean concentration profiles are self-similar throughout this zone (Morkovin 1965). The streamwise extent of this zone is from the initial zone to a distance of $18\delta_{av}$ downstream of the line source, where δ_{av} refers to the average boundary-layer thickness between the line source and the location under consideration.

The intermittent presence of ambient fluid begins to influence and reduce the growth rate of the diffusion boundary layer in the transition zone. The mean concentration profiles are no longer similar, and the value of λ/δ increases from 0.39 to 0.64. Lastly, in the final zone, the diffusion layer has spread across the momentum boundary layer. λ/δ is constant with a value of 0.64, and the mean concentration profiles are once again similar. This occurs approximately $60\delta_{av}$ downstream of the line source. Contaminant concentration levels are inversely proportional to the boundary-layer thickness, indicating that dilution by the entrained ambient fluid

determines how the concentration varies with distance from the injection slot in the final zone.

A number of investigations in the past twenty years have been aimed at acquiring an understanding of drag-reducing polymer diffusion from a line source in a TBL. Mean concentration profiles of wall-injected polymers have been measured by Wetzel & Ripkin (1970) in an open channel facility, and by Latto & El Reidy (1976) and Vdovin & Smol'yakov (1978, 1981) in a flat-plate TBL. In these studies, small total head tubes were used to draw off samples at various locations in the TBL. Fruman & Tulin (1976) investigated how diffusion reduces the polymer concentration at the wall in a flat-plate TBL. These measurements were made by drawing off samples through narrow slits in the plate surface.

The above studies indicated that the polymer solutions diffuse at a slower rate than that of a passive contaminant. The initial and intermediate zones are the most affected by the polymer, with the initial zone being appreciably lengthened relative to that of a passive contaminant. Drag reduction levels were dependent on the distance from the injector, the injected polymer concentration, the injection rate, and the free-stream velocity. Latto & El Reidy (1976) and Wetzel & Ripken (1970) found that the mean polymer concentration profiles in the final diffusion zone were similar to those of a passive contaminant. Vdovin & Smol'yakov (1978, 1981) reported that the polymer wall concentration in the intermediate and final zones could be predicted by an exponential and a power-law relation respectively. Latto & El Reidy (1976) found that their normalized diffusion boundary-layer thickness values, λ/δ, reached a constant value of only 0.46 in the final diffusion zone. However, the measurement techniques used in the above studies have been shown to give lower mean concentrations than actually exist, owing to the dependence of the solution viscosity on the polymer concentration and the magnitude of the measured concentrations being dependent on the sampling rate, see Latto, El Reidy & Vlachopoulos (1981).

Recently, a non-intrusive laser-induced-fluorescence (LIF) concentration measurement technique, developed by Koochesfahani & Dimotakis (1985), has been used to measure polymer concentration profiles. This technique offers better spatial and temporal resolution than the probe techniques mentioned above. Thus, polymer concentration profile statistics as well as a description of the dynamics of the diffusion process can be determined. Walker & Tiederman (1989, 1990), using this approach, measured polymer concentration profiles in a low-speed fully developed turbulent channel flow. Brungart *et al.* (1991) studied the diffusion of polymer in a two-dimensional flat-plate TBL with a similar procedure. Results of these studies showed that the diffusion rate of the injected polymer was significantly lower than for a passive contaminant and the initial diffusion zone was appreciably lengthened by the polymer.

Walker & Tiederman (1988) extended their polymer concentration work to include two-component laser-Doppler velocimetry (LDV) measurements with polymer injection. Additionally, the correlation between the vertical component velocity fluctuations and the concentration fluctuations, $\overline{vc}$, was measured. Their results showed a significant decrease in the vertical velocity component r.m.s. fluctuation levels and the Reynolds stress levels downstream of the slot with polymer injection. The R_{vc} correlation coefficient was reduced considerably near the slot and the correlation profiles became similar to the water injection profiles, but reduced in magnitude, with increasing distance from the slot.

The focus of the present research was to study the changes in the turbulence

structure of a flat-plate TBL modified by slot injection of concentrated polymer solutions. The friction velocity of the undisturbed flow, the injection rate of the polymer, and the streamwise distance surveyed from the slot in inner variables were an order of magnitude larger, approximately, than in the channel flow studied by Walker & Tiederman (1988, 1989). Two-component, coincident LDV measurements were made downstream of a slot injector with and without polymer injection. Boundary-layer turbulence data are presented and an interpretation of the changes in the turbulence structure resulting from polymer injection is given in light of polymer concentration profile data from LIF measurements and integrated skin friction reduction results measured with a drag balance.

2. Experimental apparatus and procedures

The experiments involving LDV and LIF measurements were conducted in a closed-loop water tunnel with a 0.76 m long by 0.305 m diameter axisymmetric test section at the Applied Research Laboratory, Penn State University. Turbulence management is achieved by a 152 mm thick honeycomb section followed by a 9:1 contraction to the test section. Optical access is provided on three sides of the test section by flat acrylic windows which blend smoothly into the circular walls of the test section. Integrated skin friction measurements were made in the same facility using a separate test section described below. A detailed description of the tunnel and its operating capabilities is provided in Lauchle, Billet & Deutsch (1989).

LDV and LIF measurements were made on a 19.05 mm thick flat plate, mounted on the horizontal centreplane of the tunnel test section. The plate is 1.2 m long and spans the 0.305 m of the tunnel test section. The plate leading edge is a two-dimensional version of a Schiebe form for enhanced cavitation performance and is located 0.1 m upstream of the beginning of the test section. A pitched asymmetric tail on the plate produced a slight negative angle of attack at the nose resulting in a measured zero-pressure-gradient flow over the working surface of the plate in the test section.

An injection slot is located 0.292 m downstream of the plate leading edge and spans the centre 0.152 m of the plate. The convergent injection slot had an exit width of 1.0 mm, measured along the surface of the plate, and a mean inclination angle of 25° with respect to horizontal. A small plenum in the plate below the injection slot assembly was loosely packed with a course non-metallic fibre mat to provide a uniform flow over the span of the slot assembly. A diagram of the flat plate is shown in figure 1.

The tunnel water and injection fluid were seeded with 1.5 μm mean diameter silicon carbide particles for light scattering for the LDV. The amounts of particles added to both the tunnel water and the injection fluid were carefully determined so that the injected fluid had the same particle number density as the tunnel water. A calibrated peristaltic pump was used to pump the water or polymer through the injection slot at desired flow rates. The injected fluid was pumped through a settling chamber containing an air bubble to eliminate any unsteadiness in the flow due to the pump before entering the tunnel.

The polymer used was polyethylene oxide (polyox). The polyox manufacturer quotes an average molecular weight of 5 million. The polymer was carefully prepared into 100 l batches of each concentration used. The freshly mixed polymer was allowed to hydrate for approximately two days before injection into the boundary layer to ensure complete mixing.

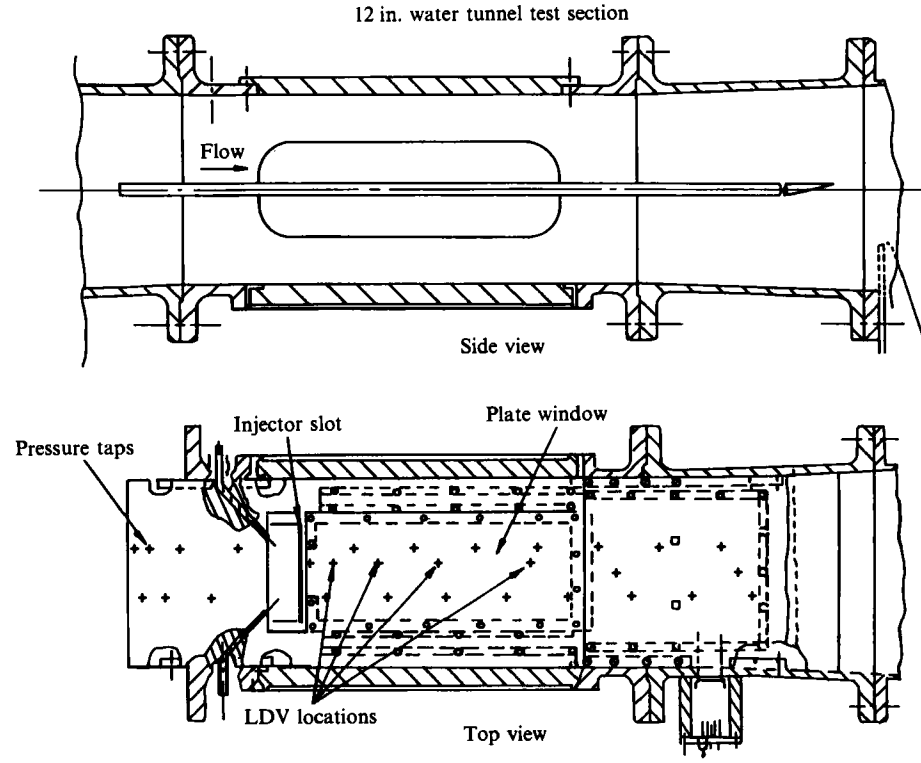

FIGURE 1. Schematic of the flat plate in the test section.

A two-colour two-component coincident fringe mode laser-Doppler velocimeter was used to survey the boundary layer on the plate. Doppler signals from the LDV were processed using counter-type signal processors. One beam in each component was effectively shifted in frequency by 2 MHz. The LDV was used in the forward-scatter mode resulting in coincident data rates of approximately 1000 bursts per s in the free stream. The LDV-determined free-stream turbulence levels were less than 0.4%, indicating a relatively clean Doppler signal. Coincidence between channels of the LDV was required for the data to be validated and transferred to the acquisition computer. The size of the time window within which data were deemed coincident was set approximately to the probe volume transit time in the free stream. Typically 25 to 50% of the data were validated as coincident.

The LDV transmitting optics were inclined approximately 2° with respect to the horizontal plane of the test plate to improve optical access. The 488 nm wavelength pair of beams of the system were in this near horizontal plane and measured the streamwise component of velocity. A beam crossing half-angle of 7.79° resulted with the 450 mm focal length lens used. This produced a probe volume diameter of 67 μm, approximately, to the e^{-2} intensity level in water. This diameter is approximately 12 wall units in the undisturbed boundary layer in the middle of the test section at a velocity $U_e = 4.5$ m/s. To reduce the angle that the LDV system had to be tilted for the optical access to measure the vertical velocity component, one of the 514.5 nm wavelength beams was directed down the optical centreline to the focusing lens. The other beam in the pair passed through the focusing lens off the centreline in a vertical plane such that the beam crossing half-angle was reduced by a factor of 2 from the

value for the 488 nm beams. The LDV transmitting and receiving optics were mounted on separate structurally sturdy bases, each with traversing capabilities. The LDV could be traversed in three directions with an uncertainty of ± 0.025 mm. The location of the plate surface was determined by visual inspection of the LDV beam crossover and the filtered Doppler signal observed on an oscilloscope as the wall was approached. The wall location could be determined with an uncertainty of approximately ± 0.05 mm.

LDV measurements were made at four streamwise positions on the centreline of the plate, at $x = 51$, 129, 232 and 384 mm from the injection slot. In inner variables at $U_e = 4.5$ m/s these locations are $x^+ = 9200$, 22600, 40300, and 66500. All LDV measurements were made at a nominal free-stream velocity of 4.5 m/s. Table 1 lists the distance of each measurement station from the slot, normalized with wall variables and with the boundary-layer thickness at the slot. The values of the friction velocity with no injection were used to normalize the distances with wall variables in table 1. The bulk of the LDV data were taken with polyox injection at $5\,Q_S$ at a 500 w.p.p.m. concentration. Limited data were also taken with injection of a 1025 w.p.p.m. solution at $2.5\,Q_S$. Q_S, the flow rate in the viscous sublayer, was 4.05 l/min/m span. LIF concentration profile measurements were taken with 500 w.p.p.m. polyox injection at various conditions.

At each streamwise position, velocity profile measurements were obtained for both no injection and injection during a single boundary-layer traverse. This was accomplished by first acquiring velocity data at a given vertical position without injection and then starting the injection system and repeating the measurement at the same vertical location in the boundary layer, then the LDV was moved to a different vertical position and the above procedure repeated until the survey was completed. Data were not taken at every location in a survey with polymer injection in order to limit polymer buildup in the free stream during the course of a survey. Adequate time was allowed between starting the injection pump and acquiring velocity data to ensure that the boundary layer had stabilized to the injection conditions.

Throughout the injection experiments, the amount of injected polymer was monitored so that the tunnel background concentration could be estimated. The tunnel was drained and refilled with polymer-free water out of large storage tanks each time the estimated background concentration of polymer approach 1 w.p.p.m. Integrated skin friction measurements from a drag-balance assembly (to be described later) indicated that a background concentration of 1 w.p.p.m. yielded a 5% reduction in measured drag. As a result, 1 w.p.p.m. was set as a limit for background polymer concentration buildup.

Data acquisition and reduction was performed on a PC/AT computer. A two-dimensional velocity inverse correction for velocity bias was applied to the LDV data before processing, see Petrie, Samimy & Addy (1988). With no injection, the friction velocity, u^*, and the pressure gradient parameter, Π, were determined by a least-squared error fit of the data to the law of the wall plus Coles wake function, see Deutsch & Zierke (1986), given as

$$u^+ = \frac{\ln(y^+)}{0.41} + 5.0 + \Delta B + \frac{\Pi}{0.41}\left(1.0 - \cos\left(\frac{\pi y}{\delta}\right)\right), \tag{1}$$

where $\Delta B = 0$ for water flow. A graphical Clauser plot routine was also used as a check for the estimated friction velocity. In all cases Π varied from 0.4 to 0.6, indicating

Meas. station	Dist. from slot X (mm)	X^+	X/δ_s	U_e (m/s)	$Re_x^\dagger$ (10^6)	Q ($\times Q_s$)	u^* (m/s)	δ (mm)	δ^* (mm)	θ (mm)	H	Re_δ^*	Re_θ
						0	0.18	5.74	0.99	0.69	1.43	4410	3090
1	50.8	9200	9.9	4.48	1.81								
						5	—	5.74	1.23	0.77	1.60	5480	3440
						0	0.18	7.29	1.20	0.84	1.43	5340	3740
2	128.6	22600	25.1	4.45	2.14								
						5	—	7.29	1.30	0.86	1.51	5790	3840
						0	0.17	8.23	1.43	1.03	1.38	6360	4600
3	231.8	40300	45.3	4.44	2.60								
						5	0.15	8.23	1.33	0.98	1.36	5910	4360
						0	0.17	10.8	1.60	1.20	1.33	7190	5390
4	384.2	66500	75.0	4.50	3.32								
						5	0.17	10.8	1.62	1.12	1.45	7290	5040

† Measured from virtual origin of boundary layer.

TABLE 1. Measured boundary-layer parameters for 500 w.p.p.m. polyox injection. The distance from the leading edge to the slot was 292.11 mm and from the virtual origin to the slot was 352.9 mm; δ_s:δ_{slot} = 5.12 mm. The uncertainties were as follows: $u^*_{Q=0Q_s} = \pm 7\%$; $u^*_{Q=5.0Q_s} = 12\%$; $\delta = \pm 0.2$ mm; δ^* and $\theta = \pm 0.1$ mm.

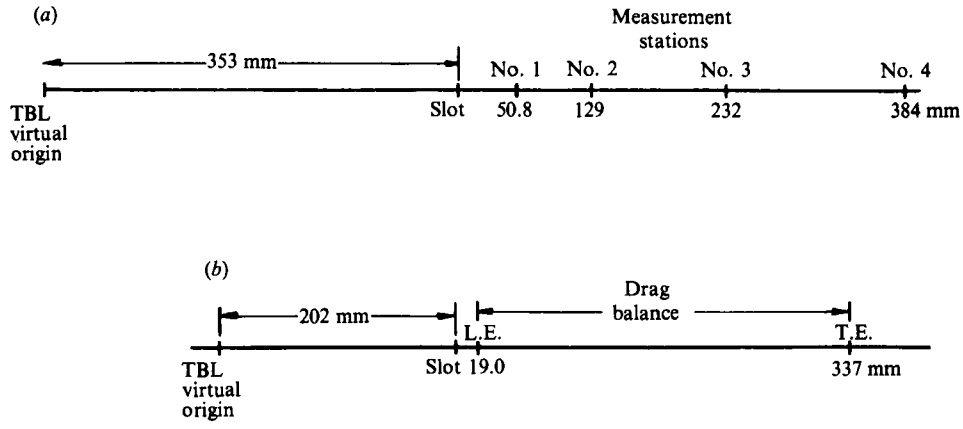

FIGURE 2. Comparison between (*a*) the axisymmetric test section flat-plate TBL and measurement locations and (*b*) the rectangular test section TBL and drag-balance location.

a zero-pressure-gradient flow. The estimated uncertainties, to the 95% confidence levels, in the evaluated u^* and Π values are $\pm 7\%$ and $\pm 14\%$ respectively.

Pressure and velocity surveys confirmed that the undisturbed TBL was a fully developed zero-pressure-gradient equilibrium flow. The pressure surveys were taken along the length of the working surface of the plate at three velocities (4.57, 9.14 and 13.7 m/s) and a nominally zero pressure gradient exists on the plate. At the key velocity, 4.57 m/s, the static pressure on the test plate changed by less than 0.2% of the dynamic head over the length of the test section.

Boundary-layer integral thicknesses given in table 1 were estimated by numerical integration of the velocity profile data using a trapezoidal method, numerical integration of a spline curve fit to the profile data, and numerical integration of (1) with the estimated values of u^* and Π, when known. Good agreement was obtained between the three methods.

An iterative procedure using both the least-squared error analysis and the Clauser plots with Π set to 0.5 was used to estimate the friction velocity and the shift in the intercept ΔB of (1) with polymer injection. However, this was possible only at the two downstream measurement locations owing to a lack of an identifiable log region in the Clauser plots of the velocity profile data at the first two measurement locations with polymer injection for the cases considered. The uncertainties in the drag-reduced value of u^* and the shift in the log-law intercept ΔB were estimated at $\pm 12\%$ and 16% respectively. In the limit of extreme flow modification by injected polymer, it is expected that the velocity profiles will approach Virk's asymptote (Virk, Mickley & Smith 1970), which has the form

$$u^+ = 11.7\ln(y^+) - 17.0. \tag{2}$$

Integrated skin friction measurements with polymer injection were performed using a drag balance in a separate rectangular test section available for this water tunnel. The TBLs that develop on the sidewall of this rectangular test section of the tunnel are similar to those on the flat plate of the axisymmetric test section, see Lauchle *et al.* (1989). Figure 2 shows a comparison of the two test sections and the distances of the TBL virtual origins and measurement locations from the injection slots. The 762 mm long rectangular test section measures 114 mm by 527 mm in cross-section. A 318 mm long by 152 mm wide flat-plate drag balance assembly is

mounted in the centre of one of the tunnel sidewalls with its leading edge located 19.0 mm downstream of a slot injector. The injection slot assembly was the same one used on the flat plate in the axisymmetric test section.

Nearly instantaneous polymer concentration profiles were determined by measuring the local intensity of the radiation emitted from a fluorescent dye premixed with the polymer prior to injection. The dye is excited to fluoresce by a laser beam that is perpendicular to the flat plate as the injectant convects through the beam. The fluorescence signal is imaged onto the input window of a single-stage microchannel plate image intensifier by a long-range microscope. The luminous gain and the electronic gating ability of the image intensifier allows snapshots of the fluorescence signal to be made with a short shutter period. A shutter period of approximately 7 microseconds was used. The output window of the image intensifier is fibre-optically coupled to a 512 element linear photodiode array. The small 25 μm centre to centre spacing of the photodiodes on the linear array combined with the 2.2 × magnification from the long-range microscope means that, ideally, a photodiode images a 2 wall unit slice of the excitation laser beam measured perpendicular to the wall at the 4.5 m/s test velocity near the middle of the test section. However, the image intensifier degrades this resolution by a factor of approximately 3 to 4. Further details concerning the procedures and apparatus can be found in Brungart (1990) and Brungart *et al.* (1991). Koochesfahani & Dimotakis (1985), and Walker & Tiederman (1988, 1989) provide similar discussions of the LIF technique. Concentration profile data of the LDV surveys are not available at station 1 but were taken upstream of this location at $x = 12.7$ mm downstream of the injection slot and at LDV stations 2, 3, and 4 listed in table 1.

3. Results and discussion

3.1. *Concentration profile results*

Mean polymer concentration profile data at $x^+ = 2350$, 22600, 40300, and 66500 with 500 w.p.p.m. polyox injection at $5Q_S$ and $U_e = 4.5$ m/s are shown in figure 3. The profile at $x^+ = 9200$ on figure 3 was not measured and is a linear interpolation estimate from the profiles at $x^+ = 2350$ and 22600. This interpolated profile is considered to be a good estimate of the actual concentration profile at this location, within 10% approximately, and is included to illustrate the expected conditions at the most upstream LDV profile location.

The curves in figure 3 show a maximum concentration located away from the wall. This error is believed to be due to a slight index of refraction gradient from the high polymer concentration near the wall and the error relaxes as the amount of polymer near the wall decreases, see Brungart *et al.* (1991). The actual wall concentrations are expected to be within 10% of these maximum values in all cases. The LDV system was not effected by the index of refraction gradients because this near-wall region was not accessible to the LDV.

Figure 4(*a*) shows the diffusion boundary-layer 50% thickness normalized by the local momentum boundary-layer thickness, λ/δ, with 500 w.p.p.m. polyox injection at $U_e = 4.5$ m/s at various injection rates. The maximum and minimum values of λ/δ with water injection over the same range of injection rates are included. The solid lines on figures 4(*a*) and 4(*b*) represent the intermediate- and final-zone results of Poreh & Cermak (1964). Figure 4(*b*) shows the diffusion-layer thickness with 500 w.p.p.m. polyox and water injection as in figure 4(*a*) but at $U_e = 9.1$ m/s. The streamwise distance, x, has been normalized by the average momentum boundary-

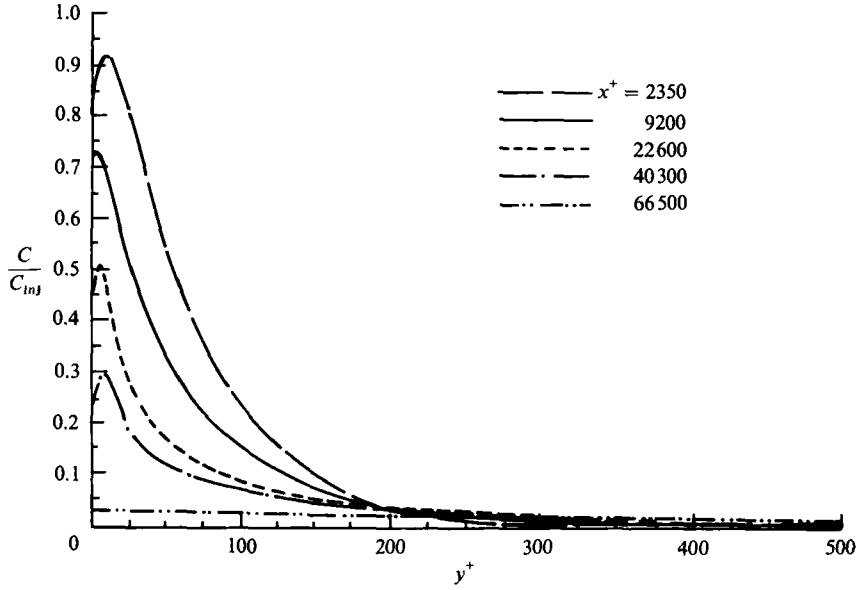

FIGURE 3. Mean polymer concentration profile data measured by LIF at $x^+ = 2350$, 22600, 40300, 66500. The $x^+ = 9200$ curve is an interpolated result

layer thickness between the slot and the measurement location, δ_{av}, as was done by Poreh & Cermak (1964). The agreement between the LIF measurements with water injection and the results of Poreh & Cermak is good and no diffusion layer-thickness dependence on injection rate was observed with water injection from 2 to 10 Q_S, (Brungart *et al.* 1991). The water injection data span the intermediate and transitional diffusion zones, and the most downstream data at $U_e = 4.5$ m/s is near the final diffusion zone.

The polymer data in figure 4 have an injection rate dependence and λ/δ decreases slowly before increasing rapidly at downstream locations. The thickness of the diffusion layer and the length of the initial diffusion zone decreases with decreasing injection rate at $U_e = 4.5$ and 9.1 m/s. These data also indicate that the length of the initial diffusion zone decreases as the free-stream velocity is increased. Generally, the values of λ/δ are smaller for $U_e = 9.1$ m/s near the slot than for $U_e = 4.5$ m/s but the opposite is true downstream.

Water-injection mean concentration profiles in the intermediate zone, normalized by the local maximum concentration, were self-similar and could be described by the empirical relationship derived by Morkovin (1965), see Brungart (1990) and Brungart *et al.* (1991). This relationship is

$$\frac{C}{C_{max}} = \exp\left[-0.693\left(\frac{y}{\lambda}\right)^a\right], \tag{3}$$

where C_{max} is the local maximum concentration, the estimated wall value, and $a = 1.5$ in the intermediate zone and $a = 2.15$ in the final zone Also, the normalized water-injection profile at $x^+ = 66500$ showed good agreement with Morkovin's curve fit of final-zone profiles.

The polymer data in figures 3 and 4(*a*) indicate that at $U_e = 4.5$ m/s the polymer maintains a concentrated layer on the wall with $\lambda/\delta < 0.1$ to $x/\delta_{av} = 34.0$ or $x^+ = 40300$. These low λ/δ values are indicative of initial-zone behaviour. The

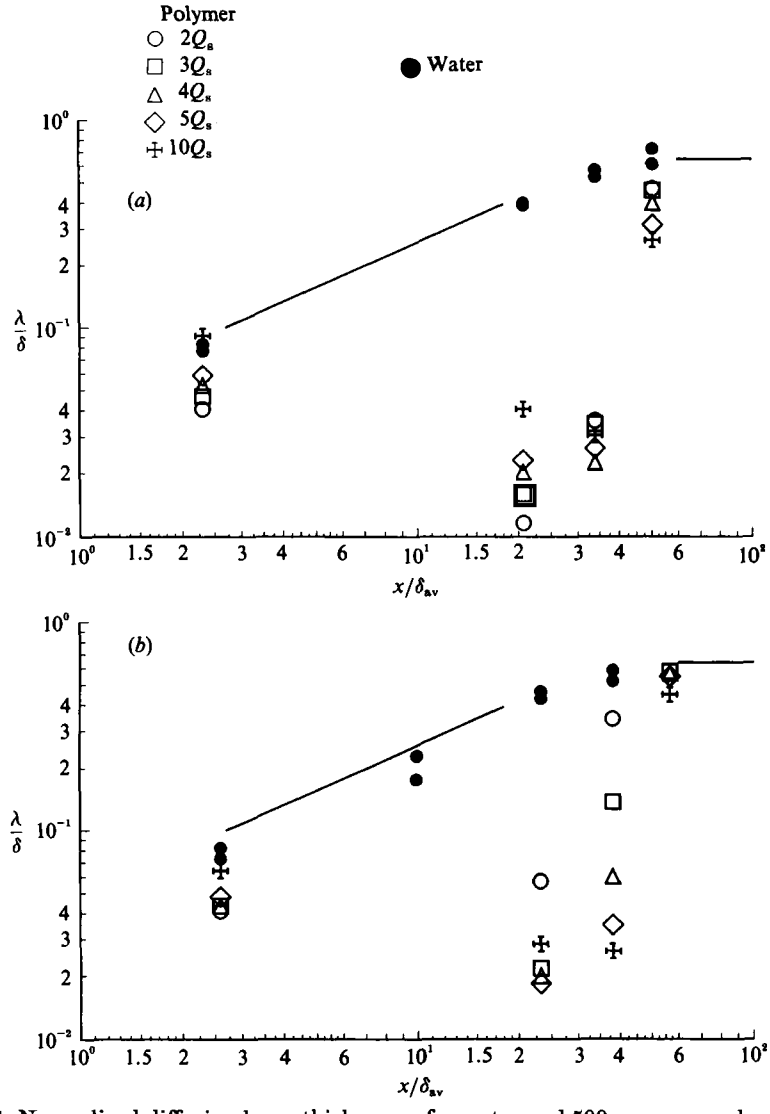

FIGURE 4. Normalized diffusion layer thicknesses for water and 500 w.p.p.m. polyox injection with (*a*) $U_e = 4.5$ m/s and (*b*) $U_e = 9.1$ m/s. The solid curve represents the passive contaminant results from Poreh & Cermak (1964) in the intermediate and final diffusion zones.

injection rate dependence of λ/δ is believed to be an initial-zone characteristic and not a behaviour unique to the polymer. The value of λ/δ for the polymer at $5Q_S$ at the last measurement location, $x^+ = 66500$, corresponds to the intermediate diffusion zone. However, the mean polymer concentration profile at this location does not agree with (3), as shown in figure 5. The mean concentration profile taken with 500 w.p.p.m. polyox injection at this same location, but with the flow rate $Q = 10Q_S$ and $U_e = 9.1$ m/s, is nearly the same. Mean concentration profiles taken at lower injection rates with $U_e = 9.1$ m/s are observed to approach the intermediate-zone curve in form. It is felt that the probe sampling techniques used in past studies failed to observe profiles of the form shown in figure 5 owing to the physical size of the probe and sampling bias that favours low concentration as mentioned in the

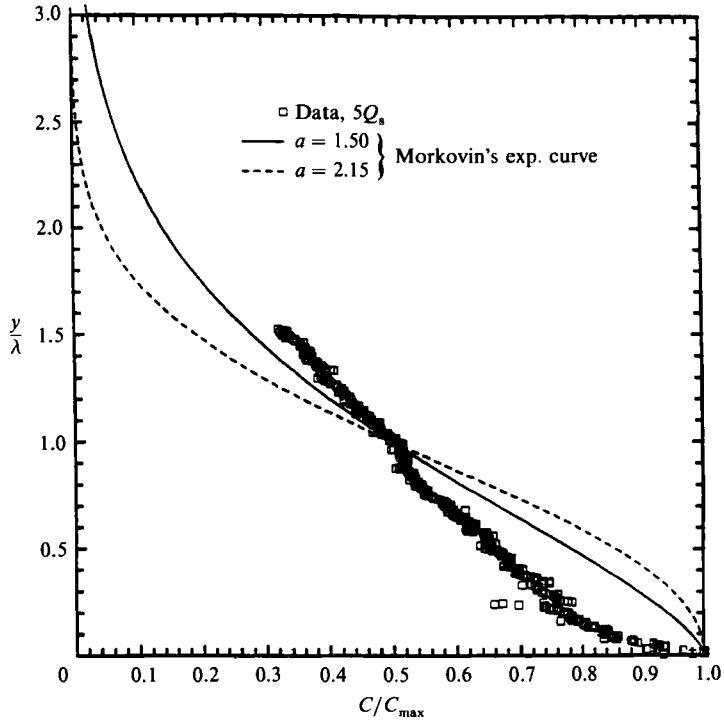

FIGURE 5. Normalized mean polymer concentration profile at $x^+ = 66500$ with $U_e = 4.5$ m/s and $C_{inj} = 500$ w.p.p.m. compared with (3), the empirical curves from Morkovin (1965).

Introduction. However, some of the concentration profile data of Wetzel & Ripken (1970) are similar. Concentration profiles similar to the polymer data in figure 5 were seen with water injection by Sommer & Petrie (1991) at the $x^+ = 9200$ location in the same facility but in a TBL modified with a large-eddy break-up device. It was concluded in Sommer & Petrie (1991) that profiles of this form are typical of the diffusion layer at the end of the initial diffusion zone.

The increase in λ/δ in figure 4 downstream of $x^+ = 40300$ is the result of the loss of a concentrated polymer wall layer by $x^+ = 66500$, as can be seen in figure 3, and does not reflect a dramatically increased rate of polymer diffusion into the outer part of the boundary layer. The distance between the two downstream stations is approximately $16\delta_{av}$ at $U_e = 4.5$ m/s, where the boundary-layer thickness is based on the values at these downstream locations. For a passive contaminant, the combined length of the initial and intermediate diffusion zones is $18\delta_{av}$. Therefore, it appears that polymer and water diffusion-layer growth rates are similar after the loss of the initial diffusion zone even though the polymer concentration profiles deviate from those of the passive contaminant. The passive contaminant definitions of these diffusion zones, insofar as the distance from the injection slot is concerned, do not seem appropriate for the polymer injection data.

By $x^+ = 40300$, the wall concentration of the polymer has dropped to approximately $0.3\,C_{inj}$, see figure 3, and significant amounts of polymer have been lost from the thin layer on the wall. The rapid decrease in the wall concentration and the corresponding high rate of polymer loss from the near-wall region appear to be maintained from the injection slot until there is no longer a sufficient supply of polymer near the wall to sustain it.

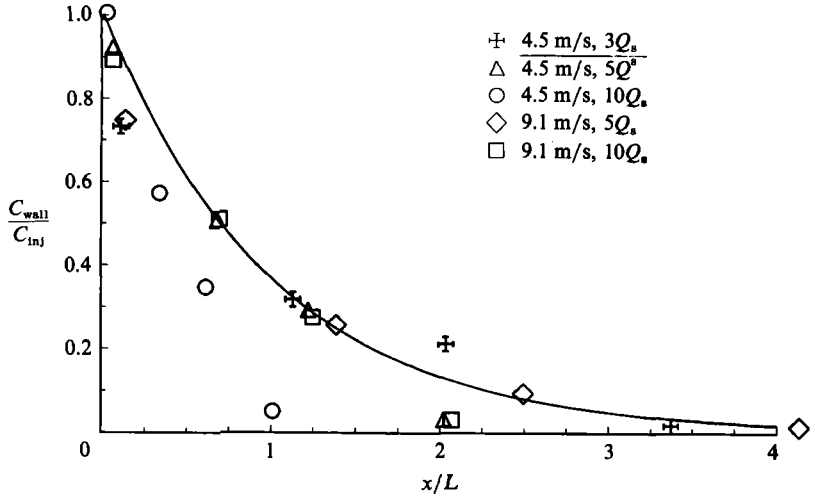

FIGURE 6. Estimated wall concentration as a function of the normalized distance from the injection slot at $U_e = 4.5$ and 9.1 m/s. Curve is equation (4) with $\kappa = 1.015$ and $\beta = -0.015$.

The decrease in the polymer wall concentration with increasing streamwise distance from the slot can be represented by an exponential relation similar to that used by Vdovin & Smol'yokav (1978):

$$\frac{C_{wall}}{C_{inj}} = \exp\left[\frac{-\kappa x}{L} - \beta\right]. \tag{4}$$

In (4), L is the distance from the injection slot for $C_{wall}/C_{inj} = e^{-1}$, and thus $\beta = 1-\kappa$. For the present results, the constants κ and β were estimated as 1.015 and -0.015 respectively, with $L = 0.19$ m. The constants representing the data of Vdovin & Smol'yakov (1978) were $\kappa = 0.7$ and $\beta = 0.3$. Since $C_{wall}/C_{inj} = 1.0$ at $x = 0$ is expected, β should be close to zero. The large value of β used by Vdovin & Smol'yakov may indicate a sampling bias as was mentioned in the Introduction. Equation (4) is valid only for $x \geqslant -\beta L/\kappa$ and $C_{wall} = C_{inj}$ upstream of this.

Figure 6 shows these concentration data versus the distance from the slot normalized with the concentration decay length, x/L, for various injection rates at $U_e = 4.5$ and 9.1 m/s. Vdovin & Smol'yakov (1978) indicate that the decay length, L, does not depend on the free-stream velocity, but in Vdovin & Smol'yakov (1981) this is said to hold only if QC_{inj} is sufficiently low. They observe that the decay length increases in proportion to QC_{inj}/U_e and that $L\rho U_e/QC_{inj}$ is a constant for a given polymer where ρ, the fluid density, is included to non-dimensionalize this variable group. Their observations are based on data taken over a range of velocities, injection rates, injection concentrations and line source locations relative to the virtual origin of the boundary layer. These results imply that the boundary-layer thickness and distance from the origin of the boundary layer are not relevant as long as the flow is fully developed at the line source. Therefore, the value of the decay length, L, for other free-stream velocities, injection rates, and injection concentrations can be estimated from the result for $U_e = 4.5$ m/s, $C_{inj} = 500$ w.p.p.m. The data in figure 6 were plotted using decay lengths determined by this approach and the agreement with (4) is generally good downstream of $x/L = 0.15$. The exceptions include the $10Q_S$ concentrations at 4.5 m/s which fall off much more quickly with increasing x/L. Vdovin & Smol'yakov (1978) observe that L does not

	Injection rate (Q_s)							
U_e (m/s)	1.6		2.4		3.2		4	
	(a)	(b)	(a)	(b)	(a)	(b)	(a)	(b)
4.5	46	49	50	49	51	50	52	51
9.1	27	48	31	48	39	49	42	49
13.7	10	37	16	45	20	45	23	48
18.3	6	21	8	28	9	32	13	35

TABLE 2. Percent drag reduction with polyox injection. Polyox concentrations: (a) 500 w.p.p.m., (b) > 1000 w.p.p.m.

increase as QC_{inj} increases indefinitely and at some point L remains fixed, and this appears to be the case for these $10Q_s$ data at $U_e = 4.5$ m/s. The other data at $x/L < 0.15$ appear to follow the same trend but this could be the result of underestimation of the wall concentration near the slot as mentioned in the discussion of figure 3.

Instantaneous polymer concentration profiles show that in the initial diffusion zone the polymer occasionally lifts off from the wall in concentrated filaments, leaving little polymer at the wall locally. This is evident in the r.m.s. concentration profile statistics where significant concentration fluctuations occur beyond $y^+ = 300$ even though mean profiles show little polymer this far from the wall. It is believed that this lifting action, which has also been observed by Walker & Tiederman (1988), plays a major role in the diffusion process in the initial diffusion zone.

3.2. *Integrated skin-friction-reduction results*

Integrated skin friction results, measured with the flat-plate drag balance in the rectangular test section, are presented in table 2. There is approximately a 52% decrease in the integrated skin friction force at the tunnel sidewall for the test conditions most similar to those studied on the flat plate with LDV – a free-stream velocity of 4.5 m/s and injection of 500 w.p.p.m. polyox solution at $5\,Q_s$. Furthermore, the data indicate that within the $\pm 5\%$ uncertainty of the balance the amount of skin friction reduction is nearly independent of the injection rate at both 500 and 1000 w.p.p.m. concentrations with $U_e = 4.5$ m/s. For 500 w.p.p.m. polyox injection at $U_e \geqslant 9.1$ m/s, the integrated skin friction decreases consistently with decreases in the injection rate. Only for $U_e \geqslant 13.7$. m/s is an injection rate dependence observed for the 1000 w.p.p.m. solution.

The trends in the integrated skin friction reduction with changing velocity, injection rate and injection concentration should behave as indicated by the result that $L\rho U_e/QC_{inj}$ is constant for a given polymer, as indicated by the observations of Vdovin & Smol'yakov (1981). Using the distance from the slot to the trailing edge of the drag balance, X_{te}, the percent drag reductions in table 2 are plotted as a function of $QC_{inj}/\rho U_e X_{te}$ in figure 7. The data fall into a band of decreasing drag reduction as $QC_{inj}/\rho U_e X_{te}$ decreases below 8×10^{-9} but the drag reduction is nearly constant at approximately a 50% level when the abscissa exceeds 8×10^{-9}. The trends are in general agreement with the anticipated scaling when $QC_{im}/\rho U_e X_{te} < 8 \times 10^{-9}$ but the results vary appreciably.

The width of the data band in figure 7 at a given value of the abscissa shows a 15% to 20% spread in drag reduction. This spread indicates that more complicated

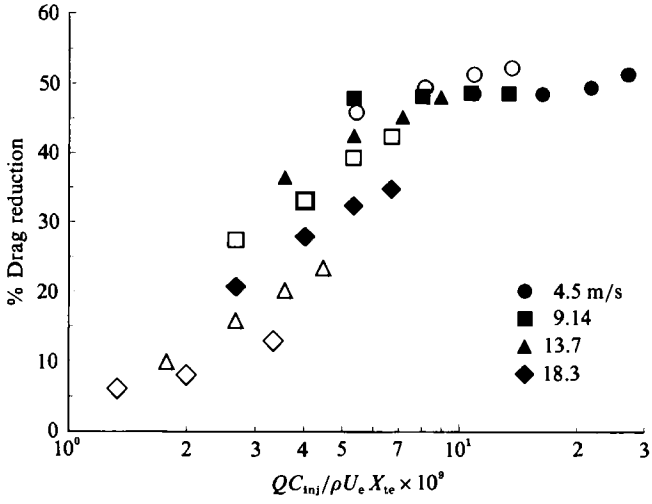

FIGURE 7. Integrated skin friction dependence on polymer injection and free-stream flow conditions. Open symbols: 500 w.p.p.m.; solid symbols: 1000 w.p.p.m.

details are involved than suggested by the scaling relationship used. The integration over the length of the drag balance may obscure some of these details. Vdovin & Smol'yakov (1981) have similar data but with miniature balances that provide a local drag reduction at a local distance from the slot. Their data, taken over a wider range of flow and injection conditions with polyox, collapse with a spread approximately half that of the current result. Other factors are likely to affect the results. For example, the 500 w.p.p.m. data at $U_e = 9.1$ m/s, the open square symbols in figure 7, should compare well with the 1000 w.p.p.m. data at 18.3 m/s, the solid diamonds. The skin friction reductions for the latter case are about 7% lower at the high velocity condition. This could be the result of shear degradation of the polymer at higher velocities.

Complicating factors that may lead to deviations from the scaling relationship include the fact that the polymer interaction with the turbulence, aside from the mass transport aspects, is likely to change with velocity. This follows from the observation of onset of drag reduction at some critical friction velocity and the decrease in friction factors with increasing Reynolds number seen in numerous homogeneous polymer pipe flow experiments. Both Virk *et al.* (1970) and Granville (1972) have used the interactive-layer concept to predict the maximum skin friction reductions possible in an external flat-plate TBL of homogeneous polymer flow as a function of Reynolds number. These Reynolds number effects on the skin friction reduction are largest at smaller Reynolds number and appear to asymptotically diminish with increasing Reynolds number (Granville 1972). Using the formulation in Virk *et al.* (1970), the maximum homogeneous skin friction reduction ranges from 51% to 60% over the length of the drag balance with $U_e = 4.5$ m/s and from 50% to 66% at $U_e = 9.1$ m/s. It is reasonable to expect a similar effect for the heterogeneous case but it should be noted that these external flow predictions have not been proven and shear degradation will have an offsetting effect.

Wu & Tulin (1972) have made similar drag-balance measurements with slot-injected polymer solutions and infer from their results that higher injection concentrations may not be as effective due to the retarded mixing that occurs initially after injection. It is generally accepted that the polymer interacts with the

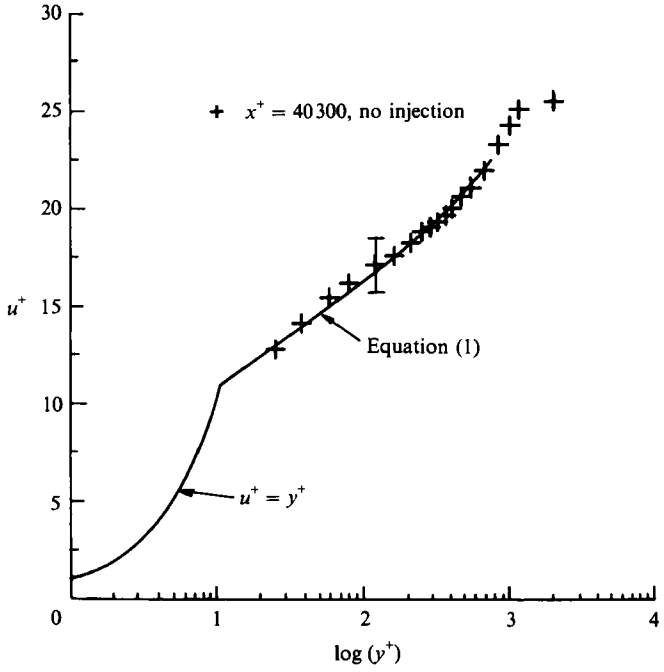

FIGURE 8. Representative mean velocity profile for the unmodified TBL.

buffer region away from the wall and therefore some mixing must occur prior to appreciable skin friction reductions. Also, higher-concentration polymer solutions have larger shear viscosities that may partially offset the effects of a reduced velocity gradient at the wall owing to the modifying actions of the polymer in the buffer region.

If the concentration decay length does not depend on the distance of the injection slot from the virtual origin of the boundary layer, as indicated by Vdovin & Smol'yakov (1981), then the concentration data taken in the axisymmetric test section are representative of the concentrations in the two-dimensional test section over the drag balance. Although this may not be a highly accurate assumption, it is generally expected that the behaviour in either test section will be similar and may help to interpret the drag balance results. The concentration results in figure 6 and the comparison between the test sections shown in figure 2 indicate that the near-wall region of flow over the drag balance is at a relatively high concentration. The mean concentration data in figure 3 indicate that the polymer concentration at the wall with 500 w.p.p.m. injection at $U_e = 4.5$ m/s exceeds 150 w.p.p.m. over a length corresponding to 70% of the distance from the slot to the drag-balance trailing edge. Of course, the effective concentration in the buffer region away from the wall is lower owing to the large concentration gradients that occur near the wall but figure 3 indicates that with $x^+ \leqslant 40300$, the concentration at $y^+ = 100$ exceeds 35 w.p.p.m.

Results presented by Wu & Tulin (1972) for homogeneous polymer solutions indicate that maximum skin friction reduction occurs at concentrations between 50 and 100 w.p.p.m. with similar polyox solutions and that the skin friction reduction increases rapidly with concentration from 0 to 30 w.p.p.m. Based on the axisymmetric test section concentration data, concentrations that produce near maximum skin friction reduction are expected near the wall over much of the drag balance at $U_e = 4.5$ m/s with 500 and 1000 w.p.p.m. injection and at $U_e = 9.1$ m/s

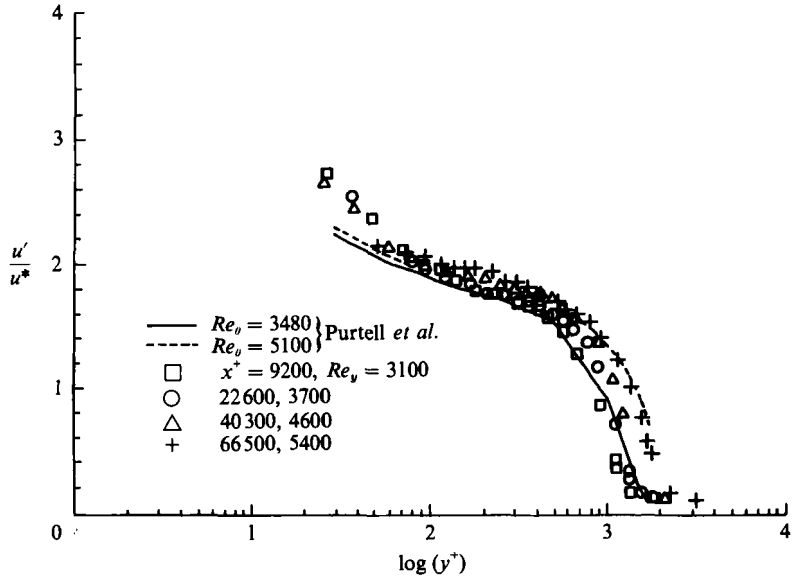

FIGURE 9. Comparison of the streamwise turbulent r.m.s. velocity profiles of the unmodified TBL with data of Purtell *et al.* (1981).

with 1000 w.p.p.m. injection. In this respect, the flow is probably saturated with polymer over much of the drag balance when $QC_{\text{inj}}/\rho U_e X_{te} > 8 \times 10^{-9}$ and the observed insensitivity to changes in the flow and injection condition results.

3.3. *No-injection velocity profile results*

Excellent agreement was obtained between profiles of the LDV mean velocity, r.m.s. fluctuation levels (denoted by a prime) and the $-\overline{uv}$ correlation data with no injection and the results of a two-dimensional zero-pressure-gradient turbulent boundary layer Klebanoff (1955), Purtell, Klebanoff & Buckley (1981), and the turbulent channel flow data of Wei & Willmarth (1989), for $y^+ > 50$. Below $y^+ = 50$, the u' levels are slightly higher, and the v' levels are approximately 5% lower, than those of Klebanoff (1955). This could be a result of the finite resolution of the LDV and the large velocity gradients near the wall, increased noise due to the proximity of the wall or from the uncertainty of the vertical displacement from the wall. A typical mean velocity profile plotted in inner variables is shown in figure 8, and the agreement with equation (1) is good. The measured streamwise r.m.s. velocity fluctuations, u', are compared with data of Purtel *et al.* (1981) in figure 9. The estimated uncertainties in the data are indicated by the error bands on a few representative points in some of the figures in the report. Table 1 lists the boundary-layer characteristics of this facility.

The velocity profile data with polymer injection are normalized with the no-injection pure water values of the friction velocity and the kinematic viscosity of water in the following discussion unless noted otherwise. This method of normalizing is for reference only and was used because of the uncertainty in and variation of the local wall shear stress and viscosity profile of the polymer-laden boundary layer. Direct comparisons of the measured quantities at the same physical distance from the surface is the result of this procedure.

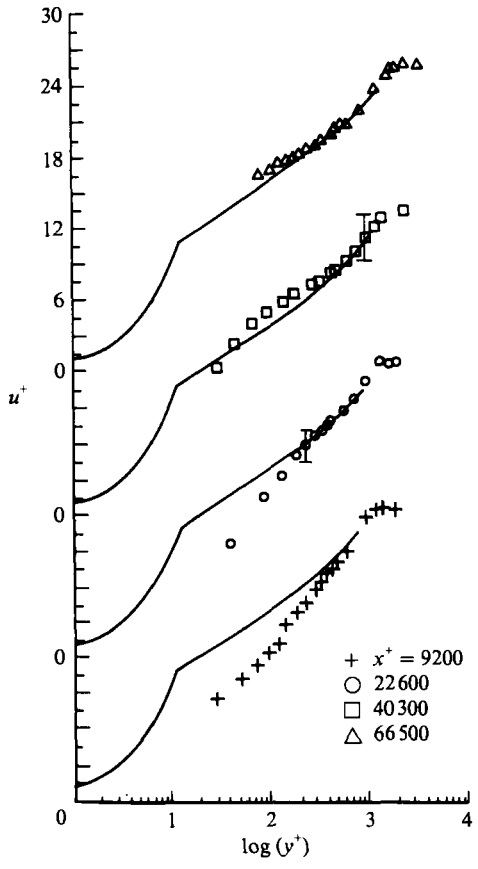

FIGURE 10. Mean velocity profiles normalized with inner variable coordinates for the polymer-injection modified TBL as a function of streamwise distance. Solid lines: no-injection represented by equation (1).

3.4. *Water-injection velocity profile results*

Water injection produced approximately a 5% increase in the vertical component r.m.s. velocity fluctuation and Reynolds stress levels near the wall, $y^+ < 100$, at the most upstream LDV survey location, $x^+ = 9200$. No effects from water injection were observed in the velocity profile statistics at the downstream locations and the no-injection and water injection profiles were the same for all statistical quantities examined. These results indicate that the injection process had a negligible influence on the turbulent boundary layer at the injection rates used and streamwise positions studied.

3.5. *Polymer-injection velocity profile results*

Figures 10 and 11 show mean velocity profiles, with and without polymer injection, plotted in inner and outer variables respectively. The solid lines in figure 10 are equation (1) fitted to the no-injection data with $u^+ = y^+$ in the viscous sublayer. Initially, the mean streamwise velocities are significantly diminished near the wall by the actions of the polymer. At $x^+ = 9200$, the resulting velocity deficit extends out to the wake region of the boundary layer even though the polymer is still primarily in a thin layer near the wall. The distance the velocity deficit extends above the surface and its magnitude diminishes with increasing streamwise distance from the

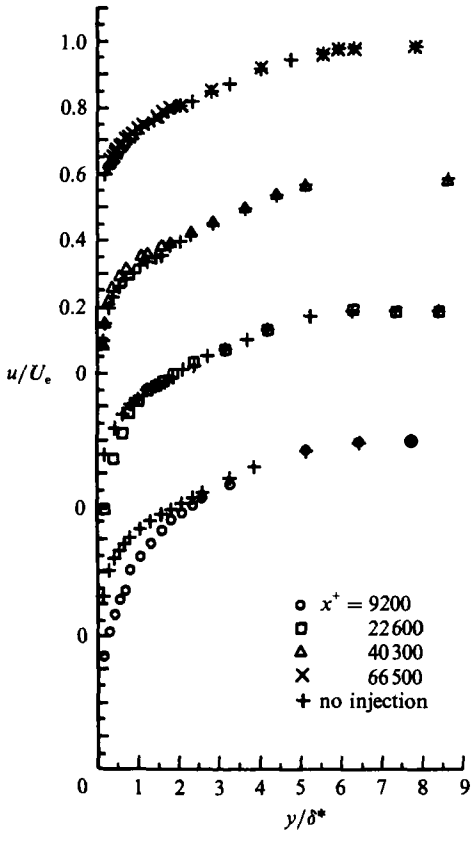

FIGURE 11. Mean velocity profiles in outer variables with and without polymer injection as a function of streamwise distance from the injection slot in inner variables, $x^+ = xu^*/\nu$.

slot as the polymer diffuses from the wall and the polymer concentration near the wall decreases. Of course, a less full velocity profile and a diminished gradient at the wall should result if significant skin friction reduction takes place. The relaxation of the mean flow velocity deficit near the wall actually appears in figures 10 and 11 to have an overshoot at the two most downstream locations. The outer region of the boundary layer, $y^+ > 500$, is unaffected at these two downstream measurement locations.

The displacement and momentum thicknesses, δ^* and θ, have increased with polymer injection compared to the no-injection values at $x^+ = 9200$, see table 1. The values of θ for the polymer-injected boundary layer are smaller than the no-injection values at the two most downstream locations and $\mathrm{d}\theta/\mathrm{d}x$ for polymer injection is lower than $\mathrm{d}\theta/\mathrm{d}x$ for the no-injection boundary layer, for $x^+ > 9200$. Since $\mathrm{d}\theta/\mathrm{d}x$ is proportional to the local wall shear stress with $\mathrm{d}p/\mathrm{d}x = 0$, a reduction in the local wall shear stress with polymer injection is indicated. The larger value of θ for polymer injection at $x^+ = 9200$ indicates that $\mathrm{d}\theta/\mathrm{d}x$ for polymer injection must be larger than the no-injection values somewhere between the slot and $x^+ = 9200$, implying either an increase in the local wall shear stress or a change in the local boundary-layer pressure gradient with polymer injection. The authors believe that the increase in $\mathrm{d}\theta/\mathrm{d}x$ occurs at or immediately downstream of the slot and that $\mathrm{d}\theta/\mathrm{d}x$ for polymer injection is lower than $\mathrm{d}\theta/\mathrm{d}x$ for the no-injection boundary layer

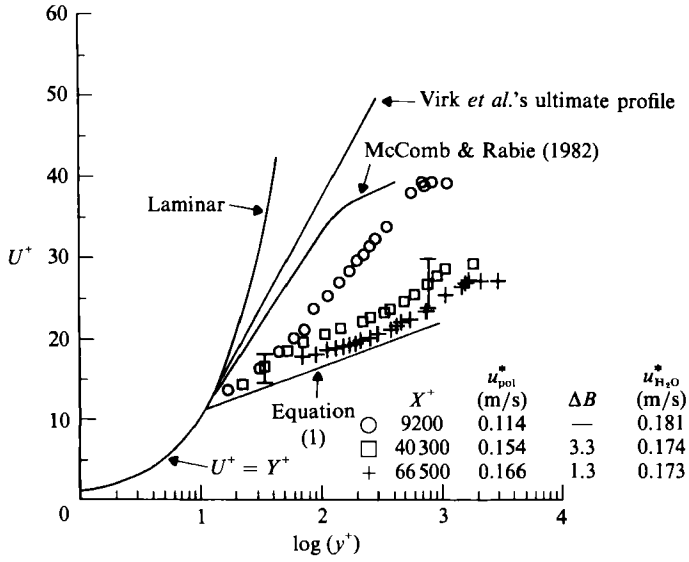

FIGURE 12. Mean velocity profiles normalized with inner variables using the estimated drag-reduced values of the friction velocity. The estimated values of u^* and ΔB are listed on the figure.

by $x^+ = 9200$. Walker *et al.* (1986) also observed an increase in the local skin friction near the location of their slot injector with polymer injection, inferred from measured pressure drop data in their fully developed turbulent channel flow study. This was probably due to slot interference and to the viscoelasticity of the polymer resulting in a swelling of the injected polymer as it exists the slot, see Fruman & Tulin (1979).

The velocity profile at $x^+ = 9200$, if normalized with the estimates for the correct values of the friction velocity (u^*) and wall value of the fluid dynamic viscosity, μ, should approach Virk's maximum-drag-reduction asymptote, see Virk *et al.* (1970). As an exercise, the profile was renormalized using a value of u^* assuming 60% skin friction reduction and replotted in wall coordinates. This estimate of skin friction reduction is within 2% of the predicted maximum value for a homogeneous polymer solution at this Reynolds number (Virk *et al.* 1970; Granville 1972). The kinematic viscosity of water was used to normalize the data. The dynamic viscosity of polyox at different concentrations was measured using a Brookfield cone viscometer. The viscosity of 100 and 500 w.p.p.m. polyox is approximately 2 and 3 times that of water, respectively. The density of polymer solutions is nearly the same as the density of the solvent fluid, in this case water. The estimated mean concentration profile at $x^+ = 9200$, see figure 3, indicates that the value of the kinematic viscosity of the solution may be slightly higher than that of water for $y^+ < 150$. As expected, the renormalized profile is approaching Virk's maximum-drag-reduction asymptote, see the $x^+ = 9200$ data in figure 12.

The ultimate profile in figure 12, which is equation (2), is a curve fit to numerous data sets for pipe flows of homogeneous polymer solutions at the condition of maximum drag reduction. Virk *et al.* suggest that this profile may be valid for flat-plate TBLs in homogeneous polymer solutions. However, this has yet to be rigorously validated for an external flat-plate flow and in particular for the external flow heterogeneous polymer-injection case of interest here. Since the laminar profile shown in figure 12 defines a limit that a TBL profile would approach, indicating

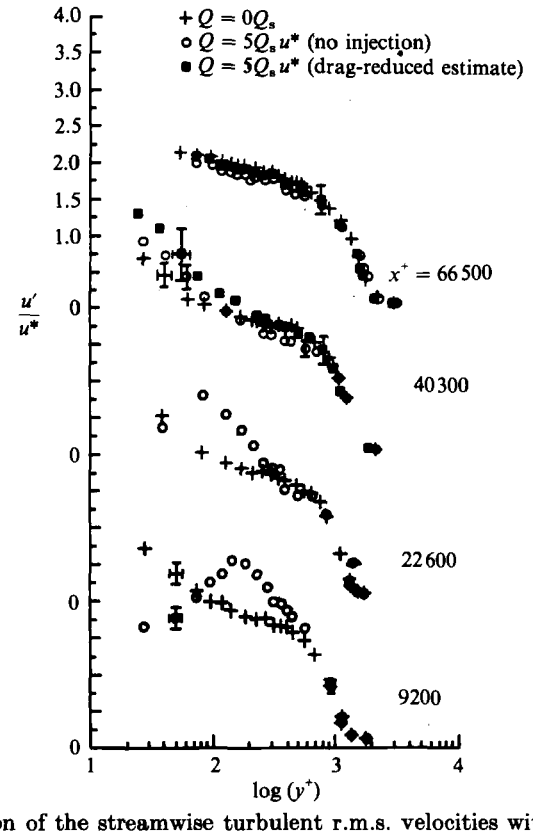

FIGURE 13. Comparison of the streamwise turbulent r.m.s. velocities with and without polymer injection at each measurement station. Solid symbols are data normalized with the estimated drag-reduced value of u^*

reversion to a laminar state, it seems plausible that TBL velocity profiles in very high-drag-reducing flows may asymptote to a profile similar to Virk's ultimate profile.

Figure 12 also shows a curve representing the mean velocity profile data from McComb & Rabie (1982) modified by wall-injected polymer. These authors made one-component LDV measurements in a pipe flow modified by wall and centreline injection of a 1000 w.p.p.m. solution of polyox WSR 301. Their wall-injection measurements were made at one streamwise location downstream of the injector, $x/r = 20.5$, where r is the pipe radius. This corresponded to an x^+ of about 80000 based on their no-injection values of u^* and ν. At this location, they obtained a 62% reduction in skin friction. Their data support the premise that a TBL, modified by wall injection of drag-reducing polymer, approaches an asymptotic mean velocity profile similar to Virk's ultimate profile.

The decrease in u^* and the increase in ΔB for the profiles at the two downstream locations in the present study, were estimated by the iterative procedure involving the Clauser plot and least-squared error analysis mentioned earlier. These downstream profiles are presented in figure 12, normalized with the estimated value of u^*. The lower polymer concentration across the boundary layer at these downstream locations justified using the viscosity of the solvent to compute y^+. The table in the inset of the figure lists the estimated values of u^* and ΔB for these profiles

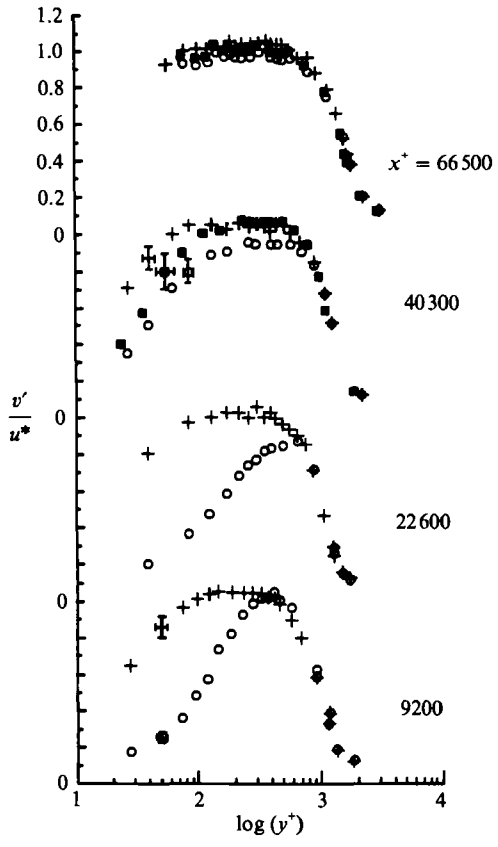

FIGURE 14. Comparison of the normal turbulent r.m.s. velocity fluctuations with and without polymer injection at each measurement station. Symbols as in figure 13.

along with the u^* values for no injection. These profiles are similar to those measured in homogeneous low-concentration polymer-ocean investigations experiencing low levels of skin friction reduction, see Reischman & Tiederman (1975) and Willmarth *et al.* (1987). It should be noted that equation (2) is not a limiting condition of (1) and that as Virk's asymptote is approached the value of κ in (1) appears to change. Just how and when κ changes is not clear. It is possible the value of κ changes only when the log region is diminished to the point that it is a negligible part of the flow, as is the case at $x^+ = 9200$. Estimation of κ as a third free parameter in (1) was attempted for the velocity profile curve fitting procedure at the two downstream locations but convergence was not achieved. It appears that κ does not deviate significantly from the classical value at these locations.

Polymer injection has a significant effect on the turbulence statistics in the boundary layer. Figure 13 shows the effect of polymer injection on the streamwise turbulent r.m.s. velocity fluctuations (u'). At $x^+ = 9200$ and 22600, u' levels are suppressed near the wall but increase to a maximum away from the wall that exceeds the local no-injection u' level significantly. The mean polymer concentrations at these u' maxima are a factor of 10 and 5 times smaller than the local concentrations near the wall, see figure 3. This u' fluctuation suppression near the wall appears to be significant only where the mean polymer concentration exceeds 15% of the injection concentration, 75 w.p.p.m. approximately. Therefore, these effects diminish

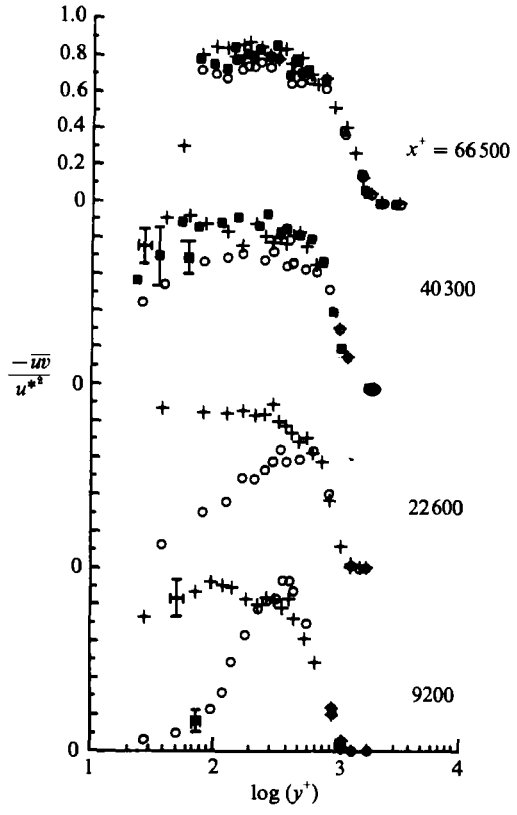

FIGURE 15. Comparison of the Reynolds shear stress profiles with and without polymer injection at each measurement station. Symbols as in figure 13.

and extend a smaller distance from the wall as the streamwise distance from the slot is increased. By $x^+ = 40300$, the polymer has diffused such that no u' suppression is evident for the data with $y^+ < 100$ but a decrease in u' levels is obtained for $y^+ > 200$. A slight suppression of u' levels is apparent over the boundary layer at the most downstream station; however, these suppression levels are within the uncertainty of the data.

Normal r.m.s. velocity fluctuation levels (v') are reduced considerably throughout most of the boundary layer at all but the most downstream location, as shown in figure 14. The v' levels decrease with increased streamwise distance from $x^+ = 9200$ to 22600 as the high-concentration polymer layer on the wall slowly diffuses out and mixes with the outer boundary layer. Unlike the reductions seen in u', significant reduction in v' levels is obtained in the outer region of the boundary layer where the mean polymer concentrations are low. The polymer concentration data at $x^+ = 22600$, figure 3, indicate that beyond $y^+ = 300$ the concentration of polymer is less than 5% of the injected concentration. However, these large v' reductions occur only where there is a noticeable layer of polymer on the wall and are much less significant at the most downstream station where the mean concentration is less than 5% of the injected concentration everywhere.

Proper scaling of the polymer data in figures 13 and 14 using the correct drag-reduced u^* values will shift the data points upward and to the left. This renormalizing produces results somewhat similar to those obtained with polymer-ocean experiments in the literature, where u' levels are increased slightly near the wall and v'

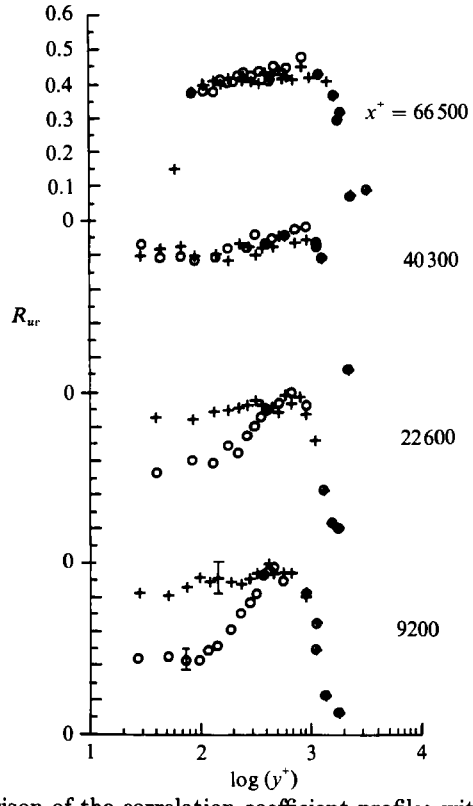

FIGURE 16. Comparison of the correlation coefficient profiles with and without polymer injection at each measurement station. Symbols as in figure 13.

levels are decreased over the boundary layer, see Willmarth *et al.* (1987) and Reischman & Tiederman (1975). These results are shown in figures 13, 14 and 15 as solid symbols at the last two downstream locations only.

Figures 15 and 16 show the effect of polymer injection on the $-\overline{uv}$ correlation and the correlation coefficient:

$$R_{uv} = \frac{-\overline{uv}}{u'v'}. \tag{5}$$

Both are significantly reduced in the inner regions of the TBL at the first two measurement locations, $x^+ = 9200$ and 22600. The Reynolds shear stress levels are lower than the no-injection values at all streamwise measurement locations while the correlation coefficient is unaffected for $x^+ > 40300$, within experimental uncertainty. At $x^+ = 9200$, a slight increase in the Reynolds shear stress level above the no-injection value was observed in the outer region of the TBL. The Reynolds shear stress profiles are similar to the v' profiles in that the Reynolds shear stress is considerably suppressed far beyond the high-concentration polymer layer near the wall. Likewise, as the polymer layer diffuses between $x^+ = 9200$ and 22600, the maximum Reynolds shear stress levels decrease. The mechanisms responsible for the v' reductions are believed to be responsible for the reduction of the Reynolds shear stress. Vertical turbulent momentum transport is reduced and this results in a decrease in skin friction. It appears that a suppression of turbulence near the wall, both u' and v', can result in a suppression of vertical fluctuations and transport all

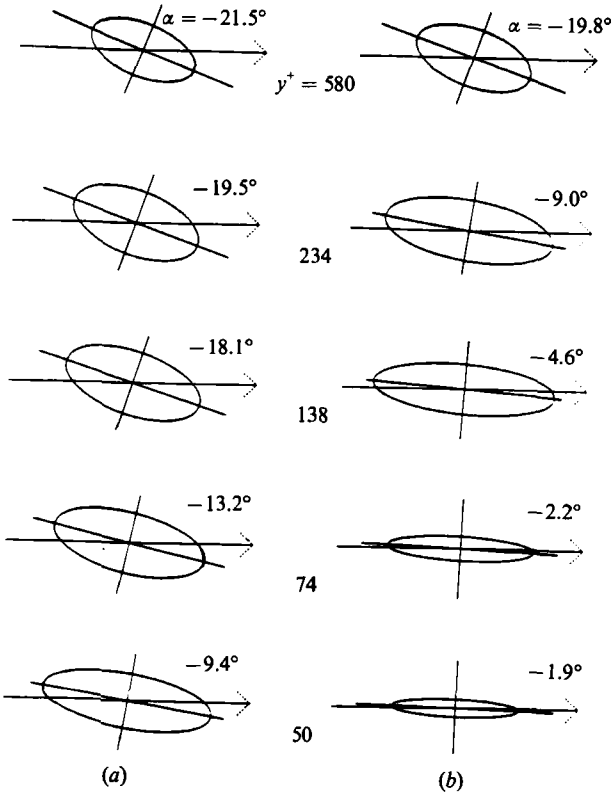

FIGURE 17. Comparison of the principal stresses in the hodograph plane with and without injection for 500 w.p.p.m. polyox at $5Q_s$, as a function of vertical distance from the wall. $x^+ = 9200$. Arrows indicate mean velocity direction. (*a*) No injection, (*b*) polyox injection.

the way across the boundary layer. This would indicate that the rotational nature of larger outer structures, that is their ability to entrain and transport fluid across the flow, may be inhibited by the near-wall modifications.

Scatter plots of the streamwise and vertical velocity fluctuations, both with and without polymer injection, indicate that as the wall is approached the principal stress axis angle, α, and the ratio of the minor-to-major principal stresses decreases. Plane stress relationships were used to reduce the data. Ellipses centred on the mean velocity with major and minor axes parallel to the major and minor principal stress axes in the fluid due to turbulent fluctuations represent the shape of the data distribution in the velocity plane well in most of the flow. Such ellipses are shown in figure 17 for both the no-injection and the polymer injection cases at $x^+ = 9200$ and at various y^+ values. The principal stress ellipses in figure 17 are drawn with major and minor axis lengths scaled equally in proportion to the size of the principal stresses. The horizontal arrow through each ellipse indicates the mean flow direction.

With no injection, the decrease in the magnitude of the principal stress angle and minor-to-major stress ratio occur across the log region of the boundary layer such that v', $-\overline{uv}$ and R_{uv} remain nearly constant. However, with polymer injection, these changes are substantial much further from the wall as shown in figure 17, and in the data on the principal stress axis angle with polymer injection in figure 18, v', $-\overline{uv}$ and R_{uv} decrease significantly. The rotation of the principal stress axis with polymer was observed qualitatively in the study by Gyr & Schmidt (1989) of joint probability

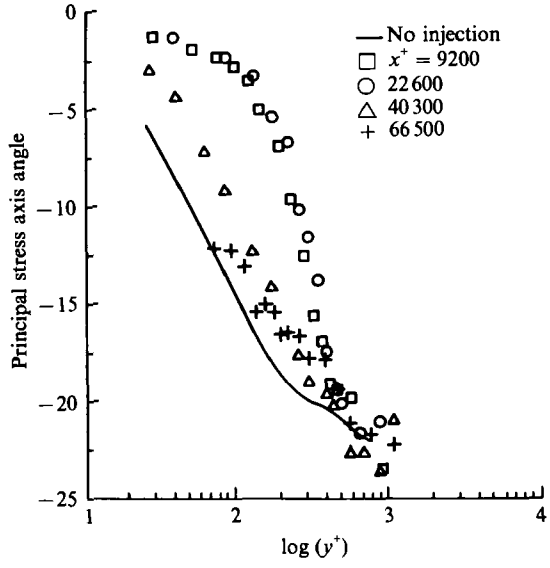

FIGURE 18. Comparison of the change in the principal stress axis angle with and without polymer injection at each measurement location.

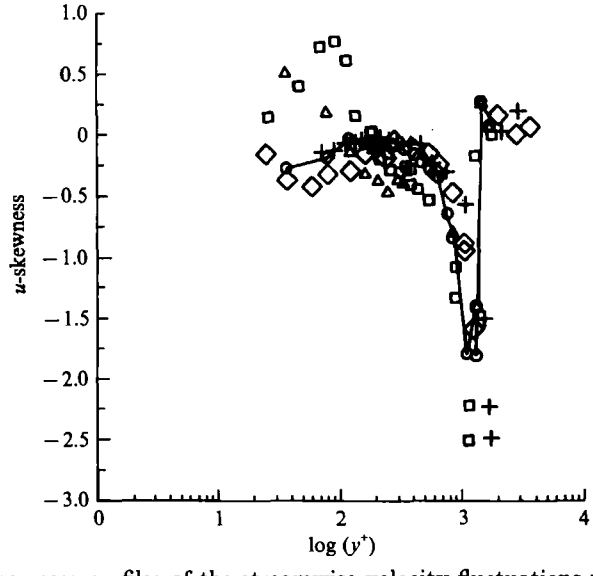

FIGURE 19. Skewness profiles of the streamwise velocity fluctuations with polymer injection. Symbols as figure 18.

distributions taken in dilute polymer pipe flow of sediment transport. Walker & Tiederman (1990) also look at joint probability distributions and these effects can be seen in their results. With polymer injection, the data distribution in the velocity plane approaches the more correlated form of a straight line. However, the correlation coefficient in figure 16 is seen to decrease substantially.

The principal stress axis results shown in figures 17 and 18 support the view that the decrease in the correlation coefficient is primarily a result of the reduction in the angle of the principal stress axis due to a suppression of the vertical velocity

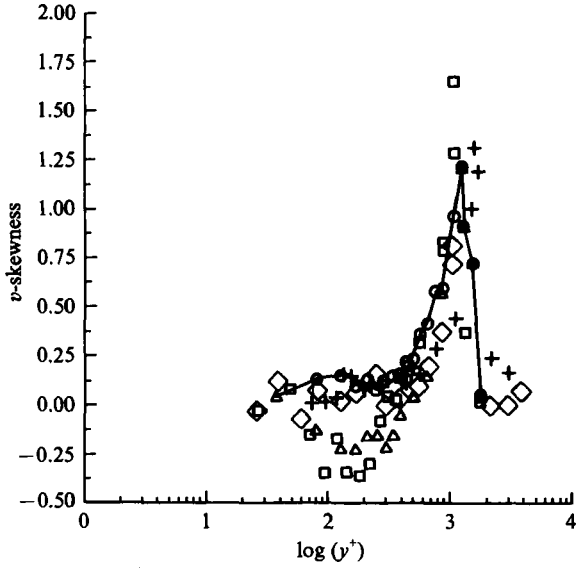

FIGURE 20. Skewness profiles of the vertical velocity fluctuations with polymer injection. Symbols as figure 18.

fluctuations for $y^+ \leqslant 300$ and is significant at the two upstream stations. At the most downstream location, the polymer-injection principal stress axis angle behaviour does not differ significantly from the no-injection data and neither do v', $-\overline{uv}$ or R_{uv}. Walker & Tiederman (1990) note that as the contributions to the Reynolds shear stress in quadrants 2 and 4 decrease owing to the changes in these stresses, contributions of opposite sign in quadrants 1 and 3 are increasing in magnitude. The combined effects are the dramatic decreases seen in the Reynolds shear stress near the wall.

Figure 19 shows the normalized third-order statistics (skewness) for the streamwise velocity fluctuations. The skewness profiles are altered by polymer injection at the nearest two measurement locations, $x^+ = 9200$ and 22600, only. At these locations, the u-distribution is more positively skewed than the water distribution near the wall, $y^+ < 200$. The u-kurtosis profiles with polymer injection have no significant differences with the no-injection profiles except for slightly larger values at $x^+ = 9200$ for $y^+ < 100$.

The skewness profiles for the vertical velocity fluctuations (v) are shown in figure 20. The v-distributions are more negatively skewed with respect to the no-injection profiles for $y^+ < 500$ at $x^+ = 9200$ and 22600. Polymer injection has a negligible effect on the skewness at $x^+ = 40300$ and 66500. Similar to the u-kurtosis profiles, the v-kurtosis profiles are nearly the same with and without polymer injection. However, v-kurtosis values are slightly higher with polymer injection at $x^+ = 9200$ and 22600 from $y^+ = 200$ to 300, indicating a more intermittent behaviour near the wall.

The positive u-skewness near the wall with polymer, where the unmodified TBL data has zero or a slightly negative skew at $x^+ = 9200$ and 22600, see figure 19, suggests that larger positive fluctuations associated with quadrant 4 sweep-type events occur with greater frequency or greater intensity than quadrant 2 lifting type events. Similarly, the negative v-skewness here shows that the motions away from the wall are relatively less intense or less frequent than with water, thus supporting the view that there is a suppression of the turbulent bursting process relative to the

sweeps. Walker & Tiederman (1990) studied polymer injection in a low-speed channel and observed that when scaled with the friction velocity, which is reduced with drag reduction, the velocity fluctuations that actually contribute the most to the Reynolds shear stress are larger with polymer injection than in the unmodified case. This was also observed by Luchik & Tiederman (1988) in a dilute polymer flow, and McComb & Rabei (1982) note that the smaller-scale fluctuations are suppressed by the polymer but the larger-scale fluctuations increase. Therefore, the primary effect of the polymer on bursting and the lifting of filaments from the wall is through reduced ejection and bursting frequencies.

The skewness and kurtosis data at the downstream locations unlike the upstream data, do not differ noticeably from the unmodified TBL. This may be a concentration effect. Luchik & Tiederman (1988) observed that the contribution to the average Reynolds shear stress during a burst is reduced with increased drag reduction in a dilute polymer channel flow. This is said to imply that the contribution of sweeps to the Reynolds shear stress must increase with drag reduction, which is what is inferred from the skewness profiles at the upstream locations in the current study.

The polymer-injection flow under study becomes significantly more dilute with increased streamwise distances and differences in the character of the modifications near the wall are indicated by the skewness data. Differences between dilute and concentrated polymer modifications are briefly mentioned by Luchik & Tiederman (1988). One difference is that the peak in u'/u^* near the wall is considerably larger at high concentrations than in the dilute case. Also, the bursting rate changes inversely with the wall streak spacing in the dilute case but at higher concentrations the decrease in the burst rate exceeds the increase in the streak spacing. This is the case with the pipe flow polymer-injection study by McComb & Rabie (1982) where the burst frequencies were lower than the Newtonian case even at the same wall shear stress. The possibility that damping of larger structures occurs at higher concentrations is mentioned as a possibility by Luchik & Tiederman (1988).

The LIF data show that the number of ejections of concentrated filaments of the injectant is reduced when the injectant is polymer compared to water at $x^+ \leqslant 22600$. Also, the average distance the filaments are ejected from the wall decreases when the injectant is polymer. Owing to mixing of the fluid that lifts off the wall, these details become difficult to discern further downstream, especially with water injection. Considering the appreciable extension of the initial diffusion zone, these results are not surprising but this does point out that the ejection of concentrated polymer filaments into the relatively polymer-free outer region of the TBL is a significant mechanism in the diffusion of the polymer from the wall and the resulting modifications to the turbulence structure in the initial diffusion zone. The initial diffusion zone and adjacent intermediate zone clearly play important roles in the effectiveness of skin friction reduction with polymer injection. Thus any model developed to describe or predict the effects of polymer injection on the TBL must adequately model the heterogeneous, intermittent mixing process of the initial diffusion zone.

These concentration and velocity profile statistic results suggest that a negative $\overline{uc}$ correlation should occur near the wall and just outside of the concentrated polymer wall layer, and that the term $\overline{vc}$ is not strongly correlated. An ejection event will produce a negative u-fluctuation, positive v-fluctuation and a positive c-fluctuation, while a sweep event will produce a positive u-, negative v- and a negative c-fluctuation. An ensemble average of the uc and vc correlation should result in a non-zero negative value for $\overline{uc}$ and a positive $\overline{vc}$. However, the v-fluctuation is

significantly reduced in the near-wall region and one suspects that the resulting $\overline{vc}$ correlation will be small. Walker & Tiederman (1988) have measured the $\overline{vc}$ correlation and have found it to be small. They observe that downward motions can carry polymer toward the wall, partially defeating the correlation. At the edge of the concentrated polymer layer on the wall, the r.m.s. levels of the u- and c-fluctuations are large and thus a significant $-\overline{uc}$ correlation could occur here. This is supported by $u\theta$ correlations where temperature is used as a passive contaminant. Antonia, Krishnamoorthy & Fulachier (1988) measured peak correlations that exceed 0.9 at $y^+ = 15$ and Chang & Blackwelder (1990) have also observed high $u\theta$ correlations near the wall.

Velocity profiles were also measured with injection of a 1025 w.p.p.m. polyox solution at an injection rate of 2.5 times the viscous sublayer flow rate. No concentration profile data are available for this injection concentration. The velocity profiles were taken at two locations, $x^+ = 22600$ and 40300. These results were very similar to those obtained with 500 w.p.p.m. polyox at 5 Q_S; however, the 1025 w.p.p.m. results were displaced downstream. The 1025 w.p.p.m. velocity profile statistics at $x^+ = 22600$ closely resembled the 500 w.p.p.m. statistics at $x^+ = 9200$. Likewise, the 1025 w.p.p.m. velocity profile statistics at $x^+ = 40300$ were similar to the statistics of the 500 w.p.p.m. profile at $x^+ = 22600$. It was anticipated that approximately doubling the polymer concentration and halving the injection rate would yield nearly identical results in the velocity field based on the scaling relationships of Vdovin & Smol'yakov (1981). As observed with the drag-balance data, the trends suggested by this scaling are generally accurate but do not completely capture all of the details that are involved.

The results of this investigation are qualitatively similar to those of Walker & Tiederman (1988). They investigated the diffusion of 700 w.p.p.m. Separan AP273 injected into a fully developed low-speed turbulent channel flow at an injection rate, per unit slot span, of 1/11.6 of the injection rate studied in the present experiment. The friction velocities they encountered are approximately an order of magnitude smaller than those encountered in the present study.

The measurements in the channel study of Walker & Tiederman (1988) covered a range of streamwise locations from $x^+ = 730$ to 5810 ($2x/h = 0.83$ to 6.7, where h is the channel height). Their results at their two downstream locations, $x^+ = 2910$ and 5810, were similar to the results obtained in the present study at $x^+ = 9200$ and 22600. Their time-resolved concentration profiles showed a streamwise region between $x^+ = 730$ to 1450 with no apparent movement of polymer, in the form of concentrated filaments, from the wall. This indicates a very significant reduction in the bursting process over this region. Furthermore, the average maximum concentration on the wall was not reduced in this region. In the present study intermittent ejections of concentrated filaments were observed at the first concentration profile measurement location at $x^+ = 2350$ ($x/\delta_{av} = 2.5$). As a result of the lack of polymer movement out of the concentrated wall layer in Walker & Tiederman's study, r.m.s. concentration profiles dropped sharply to zero outside of the wall layer and $\overline{vc}$ correlation measurements were nearly zero.

The data in Walker & Tiederman (1988) show a continual decrease in the levels of v' and $-\overline{uv}$ with increasing streamwise distance for all measurement locations, from $x^+ = 730$ to 5810. This behaviour is similar to the results obtained in this study for v' and $-\overline{uv}$ levels from $x^+ = 9200$ to 22600. A comparison of Walker & Tiederman's mean concentration profiles indicate that all their velocity profiles were measured in the initial diffusion zone of the boundary layer. In the present study, only the first

two measurement locations were well within the initial diffusion zone, the downstream location in the present study at $x^+ = 66500$ was in the latter stages of the intermediate zone, approaching the final diffusion zone. These data suggest that through most of the initial zone, decreasing levels in v' and $-\overline{uv}$ with distance can be expected.

4. Conclusions

Mean polymer concentration measurements showed a substantial lengthening of the initial diffusion zone with polymer injection. The local maximum mean concentration decreased with streamwise distance from the injection slot as described by a previously established exponential decay relationship. Time-resolved concentration profiles showed intermittent ejections of concentrated polymer filaments away from the near-wall region. It is speculated that these filaments may be partly responsible for the observed effects on the turbulence structure in the boundary layer with polymer injection. The ejection of polymer filaments are believed to be the primary diffusion mechanism in the initial zone.

Drag-balance results and LIF concentration data indicate that much of the initial diffusion zone is a region of near maximum drag reduction due to the high concentrations of polymer in the near-wall region over the length of the initial diffusion zone. As a result, integrated skin friction reduction was nearly independent of the polymer concentration and injection rate for a range of conditions. Simple scaling relationships were not completely adequate to describe measured skin friction reductions as a function of injection and flow conditions. Further investigations of the changes in the local skin friction reduction as a function of the injection and flow in combination with concentration data may clarify some of these trends.

Injection of concentrated polymer solutions into the near-wall region of a TBL causes a deceleration of the mean flow near the wall downstream of the injector. The resulting velocity deficit diminishes with increasing distance from the injector and a slight overshoot to a fuller looking mean profile downstream of $x^+ = 40300$ was observed. Considerably larger reductions in the wall-normal r.m.s. velocity fluctuation and Reynolds shear stress levels are obtained with polymer injection. At $x^+ = 9200$ and 22600, these levels are reduced significantly near the wall, and are suppressed over nearly the entire boundary layer, extending far beyond the concentrated polymer layer on the wall. Streamwise r.m.s. velocity fluctuations are suppressed near the wall owing to the high polymer concentration layer there and increase farther out in the boundary layer. The u' profile peaks at roughly the edge of the polymer layer on the wall.

The correlation coefficient, R_{uv}, is reduced substantially near the wall indicating a reduction in the contribution of the turbulent velocity fluctuations to the turbulent momentum transport, at the upstream locations. This is due primarily to the decrease in the magnitude of the angle of the principal stress axis with the suppression of vertical velocity fluctuations. The above effects diminish as the polymer diffuses from the wall.

The velocity profile statistics and the concentration measurements indicate that the TBL bursting process is suppressed by injection of polymer solutions into the near-wall region of the TBL. Based on LIF visualization of lifting polymer filaments, the polymer reduces the frequency of lifting quadrant 2 events in the initial zone. These results show clearly that turbulent transport of momentum in the direction normal to the wall is suppressed, most prominently near the wall.

Increasing the injected polymer concentration by approximately a factor of 2 and halving the injection rate produced velocity field modifications similar to the original concentration and injection rate experiments but shifted downstream. As with the integrated skin friction results, these data suggest that the details of these flow modifications do not scale simply.

The data indicate that the mean velocity profiles of TBLs experiencing high levels of polymer drag reduction will approach an asymptotic mean velocity profile. The asymptotic profile should correspond to a condition of maximum drag reduction. Whether this asymptotic profile in an external TBL with polymer injection is in fact Virk *et al.*'s ultimate profile remains to be validated. Furthermore, the maximum levels of drag reduction which can be obtained require further investigation.

The authors would like to acknowledge the support of the US Navy David Taylor Research Center, Mr W. G. Souders, Technical Monitor.

REFERENCES

ANTONIA, R. A., KRISHNAMOORTHY, L. V. & FULACHIER, L. 1988 Correlation between the longitudinal velocity fluctuation and temperature fluctuation in the near-wall region of a turbulent boundary layer. *Intl. J. Heat Mass Transfer* **31**, 723–730.

BERMAN, N. S. 1978 Drag reduction by polymers. *Ann. Rev. Fluid Mech.*, **10**, 47–64.

BRUNGART, T. A. 1990 A fluorescence technique for measurement of slot injected fluid concentration profiles in a turbulent boundary layer. Masters thesis, Department of Mechanical Engineering, The Pennsylvania State University.

BRUNGART, T. A., HARBISON, W. L., PETRIE, H. L. & MERKLE, C. L. 1991 A fluorescence technique for measurement of slot injected fluid concentration profiles in a turbulent boundary layer. *Exps Fluids* **11**, pp. 9–16.

CHANG, S. & BLACKWELDER, R. F. 1990 Modification of large eddies in turbulent boundary layers. *J. Fluid Mech.* **213**, 419–442.

DEUTSCH, S. & ZIERKE, W. C. 1986 The measurement of boundary layers on a compressor blade in cascade at high positive incidence angle. *NASA Contractor Rep.* 179492.

FRUMAN, D. H. & TULIN, M. P. 1976 Diffusion of a tangential drag reducing polymer injection of a flat plate at high Reynolds numbers. *J. Ship Res.* **20**, 171–180.

FRUMAN, D. H. & TULIN, M. P. 1979 Effects of additive ejection on lifting hydrofoils *Trans. ASME* I: *J. Fluids Engng* **101**, 244–250.

GRANVILLE, P. S. 1972 Maximum drag reduction for a flat plate in polymer solution *J. Hydronaut.* **6**, 58–59.

GYR, A. & SCHMIDT, W. 1989 Stabilization of sediment transport in pipes by drag reducing additives. In *Drag Reduction in Fluid Flows* (ed. R. Sellin & T. Moses), pp. 223–230. Ellis-Horwood.

KLEBANOFF, P. S. 1955 Characteristics of turbulence in a boundary layer with zero pressure gradient. *NACA Rep.* 1247.

KOOCHESFAHANI, M. M. & DIMOTAKIS, P. E. 1985 Laser-induced fluorescence measurements of mixed fluid concentration in a liquid plane shear layer, *AIAA J.* **23**, 1700–1707.

LATTO, B. & EL REIDY, K. F. 1976 Diffusion of polymer additives in a developing turbulent boundary layer. *J. Hydronaut.* **10**, 135–139.

LATTO, B., EL REIDY, K. F. & VLACHOPOULOS, J. 1981 Effect of sampling rate on concentration measurements in nonhomogeneous dilute polymer solution flow. *J. Rheol.* **25**, 583–590.

LAUCHLE, G. C., BILLET, M. L. & DEUTSCH, S. 1989 High Reynolds number liquid flow measurement. In *Frontiers in Experimental Fluid Mechanics* (ed. M. Gad el Hak). Lecture Notes in Engineering, vol. pp. 95–157. Springer.

LUCHIK, T. S. & TIEDERMAN, W. G. 1988 Turbulent structure in low-concentration drag-reducing channel flows. *J. Fluid Mech.* **190**, 241–263.

McComb, W. D. & Rabie, L. H. 1982 Local drag reduction due to injection of polymer solutions into turbulent flow in a pipe. Part 1: Dependence on local polymer concentration; and Part 2: Laser Doppler Measurements of Turbulence Structure. *A. AIChE*, **28**, 547–565.

Morkovin, M. V. 1965 On eddy diffusivity, quasisimilarity and chemical reactions in turbulent boundary layers. *Intl J. Heat Mass Transfer* **8**, 129–145.

Petrie, H. L., Samimy, M. & Addy, A. L. 1988 Laser Doppler velocity bias in separated turbulent flows. *Exps Fluids*, **6**, 80–88.

Poreh, M. & Cermak, J. E. 1964 Study of diffusion from a line source in a turbulent boundary layer. *Intl J. Heat Mass Transfer* **7**, 1083–1095.

Purtell, L. P., Klebanoff, P. S. & Buckley, F. T. 1981 Turbulent boundary layer at low Reynolds numbers. *Phys. Fluids* **24**, 802–811.

Reischman, M. M. & Tiederman, W. G. 1975 Laser Doppler anemometer measurements in drag-reducing channel flows. *J. Fluid Mech.* **70**, 369–392.

Sellin, R. H. J., Hoyt, J. W. & Scrivener, O. 1982*a* The effect of drag reducing additives on fluid flows and their industrial applications Part 1: Basic aspects. *J. Hydraul. Res.*, **20**, 29–68.

Sellin, R. H. J., Hoyt, J. W., Pollert, J. & Scrivener, O. 1982*b* The effect of drag reducing additives on fluid flows and their industrial applications Part 2: Applications and future proposals. *J. Hydraulic Res.* **20**, 235–292.

Sommer, S. T. & Petrie, H. L. 1991 Concentration statistics of active and passive additives downstream of a line source in a LEBU modified turbulent boundary layer. In *Laser Anemometry: Advances and Applications* (ed. A. Dibbs and B. Ghorashi) (editors), vol. 2, pp. 473–481. ASME.

Tiederman, W. G., Luchik, T. S. & Bogard, D. G. 1985 Wall layer structure and drag reduction. *J. Fluid Mech.* **156**, 419–437.

Toms, B. A. 1949 Some observations on the flow of linear polymer solutions through a straight tube at large Reynolds number. *Proc. First Intl Congress on Rheology*, vol. 11 Pt. 2, pp. 134–141. North-Holland.

Vdovin, A. V. & Smol'yokav, A. V. 1978 Diffusion of polymer solutions in a turbulent boundary layer. *Zh. Prikl. Mekh. Tekh. Fiz.* **2**, 66–73 (transl. in UDC 532.526, pp. 196–201, Plenum).

Vdovin, A. V. & Smol'yokav, A. V. 1981 Turbulent diffusion of polymers in a boundary layer. *Zh. Prikl. Mekh. Tekh. Fiz.* **4**, 98–104 (transl. in UDC 532.526 (1982) pp. 526–531. Plenum).

Virk, P. S., Mickley, H. S. & Smith, K. A. 1970 The ultimate asymptote and mean flow structures in Toms' phenomenon. *Trans. ASME* E: *J. Appl. Mech.* **37**, 488–493.

Walker, D. T. & Tiederman, W. G. 1988 Turbulent structure and mass transport in a channel flow with polymer injection, *Rep.* PME-FM-22-2. Purdue University.

Walker, D. T. & Tiederman, W. G. 1989 The concentration field in a turbulent channel flow with polymer injection at the wall. *Exps Fluids* **8**, 86–94.

Walker, D. T. & Tiederman, W. G. 1990 Turbulent structure in a channel flow with polymer injection at the wall. *J. Fluid Mech.* **218**, 377–403.

Walker, D. T., Tiederman, W. G. & Luchik, T. S. 1986 Optimization of the injection process for drag reducing additives. *Exps Fluids* **4**, 114–120.

Wei, T. & Willmarth, W. W. 1989 Reynolds-number effects on the structure of a turbulent channel flow. *J. Fluid Mech.* **204**, 57–95.

Wetzel, J. M. & Ripken, J. F. 1970 Shear and diffusion in a large boundary layer injected with polymer solution. *Project Rep.* 114. St. Anthony Falls Hydraulic Laboratory, University of Minnesota.

White, A. & Hemmings, J. A. C. 1976 *Drag Reduction by Additives: Review and Bibliography.* Cranfield [Eng], BHRA Fluid Engng.

White, F. M. 1974 *Viscous Fluid Flow*, McGraw Hill.

Willmarth, W. W., Wei, T. & Lee, C. S. 1987 Laser anemometer measurements of Reynolds stress in a turbulent channel flow with drag reducing polymer additives, *Phys. Fluids* **30**, 933–935.

Wu, J. & Tulin, M. P. 1972 Drag reduction by ejecting additive solutions into a pure water boundary layer. *Trans. ASME* D: *J. Basic Engng* **94**, 749–755.